

Confidential Prompting: Protecting User Prompts from Cloud LLM Providers

In Gim*, Caihua Li*, Lin Zhong

Department of Computer Science

Yale University

{in.gim, caihua.li, lin.zhong}@yale.edu

* Both authors contributed equally

Abstract—Our work tackles the challenge of securing user inputs in cloud-hosted large language model (LLM) serving while ensuring output invariance, model confidentiality, and compute efficiency. We introduce *secure multi-party decoding (SMD)*, which leverages confidential computing to confine user prompts to a trusted execution environment (TEE), namely a confidential virtual machine (CVM), while allowing service providers to generate tokens efficiently. We also introduce a novel cryptographic method, *prompt obfuscation (PO)*, to ensure robustness against reconstruction attacks on SMD. We demonstrate that our approach preserves both prompt confidentiality and LLM serving efficiency. Our solution can enable privacy-preserving cloud LLM serving that handles sensitive prompts, such as clinical records, financial data, and personal information.

1. Introduction

Large language models (LLMs) are often hosted on cloud platforms, which introduces privacy concerns as prompts can include sensitive data, ranging from personal communications to health information. Not surprisingly, many IT, financial and healthcare industries, wary of information breaches, restrict the usage of cloud LLM at work [1], [2]. Privacy concerns also subject cloud-hosted LLM services to regulations like GDPR and HIPAA [3], [4] and, as a result, hamper their adoption. Cloud-hosted LLM services further raise intellectual property (IP) concerns because prompts are increasingly recognized as IPs, with emerging marketplaces for them. Both privacy and IP concerns underscore the importance of safeguarding prompt confidentiality in cloud environments.

This paper aims at *confidential prompting* in cloud-hosted LLM services, which achieves the confidentiality of user prompts while meeting three crucial constraints for commercial LLM service: output invariance, model confidentiality, and compute efficiency. *Output invariance* guarantees that the output of the LLM service remains the same regardless of whether confidentiality measures are applied to the prompts, ensuring the utility and reliability of the service. *Model confidentiality* ensures that the LLM’s model weights are kept secret from users. *Compute efficiency* requires that the introduction of confidentiality measures does not significantly increase the service cost. As a first step, we consider the

Honest-but-Curious (HBC) threat model, in which the LLM provider faithfully follows all computation steps for LLM inference but tries to extract as much information as possible from the user.

As we will present in §2.2 and §2.4, none of existing solutions meet all of these constraints. For example, differentially private in-context learning (DP-ICL) [5], [6] and data anonymization [7], alter the output, thus violating output invariance. Techniques like edge inference [8] and multiparty computation (MPC) [9] protect input by processing them locally in part, but this approach requires sharing some LLM weights with the user, which undermines model confidentiality. Although fully homomorphic encryption (FHE) [10], [11] preserves both output invariance and model confidentiality, its extensive computational demands restrict its feasibility for LLMs. More recently, Confidential Computing (CC) [12] has emerged as a promising approach to secure cloud-based DNN [13], [14], [15], particularly through the use of confidential virtual machines (CVMs) with GPU support. Although CVMs can ensure output invariance and model confidentiality, their naive applications demand complete trust in the LLM provider or prove impractical for LLM serving, due to the large memory footprint of LLMs within user CVMs, which limits scalability due to GPU memory constraints, and to the lack of batch parallelism.

This work presents a new approach to confidential prompting that uses CVMs in an efficient and scalable manner, illustrated by Figure 1. Our key insight is that the delivery of LLM involves two distinct phases: prefill and decode, and the latter dominates computational use. Our approach, called *Obfuscated Secure Multi-party Decoding (OSMD)*, implements prefill inside per-user CVMs and keeps the resulting KV attention states (called private KV cache) there, because prefill requires the plaintext prompt and the private KV cache can be used to reconstruct the prompt. OSMD then implements decode mostly outside the CVMs, without disclosing the private KV cache, using a technique called *Secure Multi-party Decoding (SMD)* (§4).

SMD formulates token generation (decode) as a secure two-party computation with one party being the CVM and the other the LLM provider: only the latter needs the LLM weights for decoding. The CVM already has the private KV cache from prefill and no longer requires any LLM weights for decode. On the other hand, the LLM provider computes

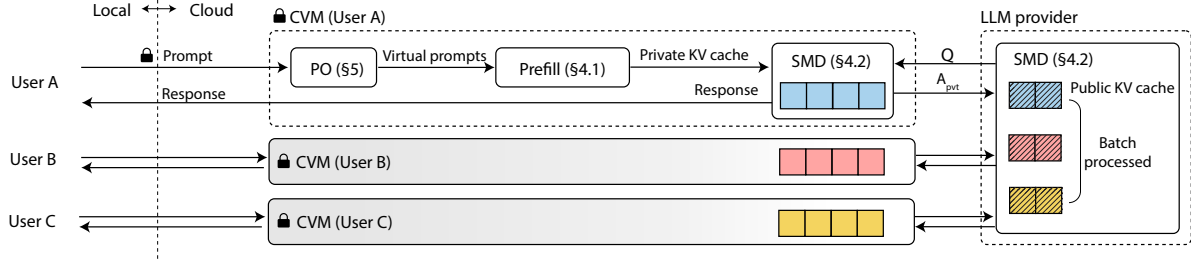


Figure 1: **Overview of Confidential Prompting by OSMD.** A user and their CVM collaborate to protect the user’s prompt from the LLM provider by applying Secure Multi-party Decoding (SMD) and Prompt Obfuscation (PO). The user prepares their prompt on a local machine, while the user’s CVM and the LLM provider are hosted in the cloud. PO occurs within the CVM during the prefill phase, while SMD involves both the CVM and the LLM provider during decoding.

the KV attention states for the newly generated tokens as the public KV cache. During the interaction between the CVM and the cloud LLM, the CVM computes the private attention score (A_{pvt}) with the private KV cache, and provides it to the LLM provider without exposing the private states. This enables the LLM provider to compute the final attention score and generate new tokens, without compromising output invariance. This partitioning approach is efficient because (1) the CVM does not have to retain the LLM model weights after prefill, and (2) the LLM provider can batch process the public attention states in parallel.

OSMD overcomes two challenges to SMD. First, SMD is vulnerable to (semi) black-box reconstruction attacks that approximate the private states with observations of the interaction and compromise prompt confidentiality. To address this, we introduce a novel cryptographic method, *prompt obfuscation (PO)* (§5), inspired by *chaffing and winnowing* (§2.3). The user’s CVM generates fake n-grams that appear as authentic as the original segments in the user’s prompt. The CVM uses these fake n-grams to create a set of *virtual prompts*. The LLM provider is responsible for generating tokens for the authentic prompt and each virtual prompt in parallel, but the CVM only relays the generated tokens of the only authentic prompt back to the user. We offer a formal analysis of the security provided by PO in §5.3, as well as a memory-efficient algorithm to serve multiple virtual prompts within the CVM. Second, prefill, performed within the CVM, requires LLM weights and as a result, may jeopardize model confidentiality. OSMD addresses this issue by allowing the LLM provider to check the integrity of the transferred output tokens, ensuring that the malicious client cannot exfiltrate LLM weights by sending arbitrary bytes. The cloud vendor can also limit the outbound traffic to only what is necessary to transmit the generated tokens. See §4.1.

In §6, we report an implementation of OSMD (SMD+PO) using PyTorch. In §7 we evaluate our prototype on NVIDIA H100 GPU, with GPU CC enabled, against two naive CVM-based solutions (Figure 2b and Figure 2c). We show that OSMD achieves 5× better latency than the naive CVM-based solution that defends against cloud LLM providers and scales well to (1) the number of concurrent users, (2) the size of the model, and (3) the number of input/output tokens. In §8, we

conclude our work, discuss its limitations and what it takes to achieve stronger protection. For instance, SMD requires a weaker adversary model, i.e., HBC, compared to serving entirely in CVMs. Also, the effectiveness of PO is conditional, although we can detect potential information leaks and alert the user of such cases. We believe that cloud LLM serving that is both privacy-preserving and efficient is important and timely. Our work marks the first step towards utilizing confidential computing for secure LLM serving, and we hope it will spark further discussion on confidential prompting and methods offering stronger protection. We open-source OSMD in github.com/yale-sys/confidential-prompting.

2. Background and Related Work

We design Confidential Prompting on top of the *Key-Value (KV) Cache* mechanism, i.e., reusing the key-value attention states in autoregressive decoding. It leverages *confidential computing* techniques to protect the private KV cache. Its design of *prompt obfuscation* is inspired by the design of *chaffing and winnowing*. We next provide a succinct background about these mechanisms and techniques.

2.1. LLM Inference with KV cache

2.1.1. Tokens. A token is an atomic unit of text that the LLM processes, representing parts of words, entire words, or even punctuation. The exact breakdown into tokens depends on the model’s tokenization algorithm, which converts a string into a sequence of tokens. For example, a sentence like “The cat sat” might be tokenized as (“The”, “cat”, “sat”), while more complex words can be split into multiple tokens (e.g., “unbelievable” becomes (“un”, “believ”, “able”)). The typical size of a token vocabulary ranges from 12K to 128K.

2.1.2. LLM Inference. We consider GPT-style LLMs [16], [17], [18], [19], which are trained to predict the distribution of the next token, s_{n+1} , given a sequence of tokens s_1, \dots, s_n , known as causal language modeling. This prediction process uses the Transformer architecture [20], which consists of multiple self-attention layers. For a sequence of length n , represented as $X \in \mathbb{R}^{n \times d}$, the Transformer produces an

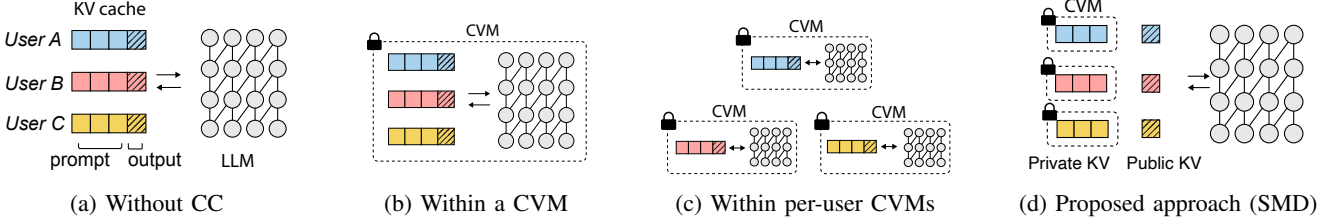


Figure 2: **Various LLM serving approaches.** (a) LLM serving without confidential computing (CC) is the most efficient, but user prompts are exposed to both the cloud infrastructure and the LLM provider, as well as any adversaries that may compromise the cloud. (b) Serving multiple users with a single CVM can protect against malicious cloud provider and adversaries on the cloud, but prompts remain exposed to the LLM provider. (c) Assigning a separate CVM per user offers higher level of protection, from both cloud infrastructure and LLM provider, but it is inefficient since each CVM contains its own copy of the LLM. (d) SMD strikes a balance between security and efficiency by isolating only the user’s prompt (and private KV cache) within the CVM, while allowing batch processing across users.

output sequence $Y \in \mathbb{R}^{n \times d}$, where d is the hidden dimension size. The self-attention mechanism, a core component of the Transformer, requires five matrix multiplications. First, the model computes matrices $Q = XW_Q$, $K = XW_K$, and $V = XW_V$, where W_Q , W_K , and $W_V \in \mathbb{R}^{d \times d}$ are trainable weight matrices. Next, the output is calculated as $Y = \sigma(QK^\top)V \in \mathbb{R}^{n \times d}$, where $\sigma(\cdot)$ denotes the softmax function. The output becomes an input to the next self-attention layer. The LLM samples the next token s_{n+1} from the distribution and appends it to the token sequence, iteratively until some termination condition is met, so called autoregressive token generation.

2.1.3. KV Cache. The KV cache mechanism [21], [22], [23], [24] is a technique frequently used to improve LLM inference efficiency. This mechanism leverages the causal nature of LLMs: when predicting a token s_i within an input token sequence, the attention computation only considers preceding tokens, s_1, \dots, s_{i-1} , rather than any tokens that follow. Consequently, instead of recalculating attention for all tokens in the input at each generation step, the LLM inference engine “caches” previously computed attention states and reuses them for subsequent inferences. Since the reusable attention states consist of the K and V tensors for each token, this technique is referred to as KV caching.

2.2. Confidential Computing and Inferencing

2.2.1. Confidential Computing. Confidential computing protects *data in use*, complementing traditional security measures such as encryption that protect *data at rest* and *data in transit*. The most common approach to confidential computing is the use of trusted execution environments (TEEs), such as enclaves and confidential virtual machines (CVMs), which are provided by hardware features like AMD SEV [25] and Intel TDX [26]. These environments isolate sensitive data and code. Thanks to their strong isolation capabilities, hardware-based TEEs ensure that even privileged entities such as the OS and hypervisor cannot access the data being processed. In addition to isolation, most hardware-based solutions also provide runtime encryption and remote

attestation. Runtime encryption guarantees that all data and code within a CVM (or enclave) are encrypted in memory, offering an additional layer of protection. Remote attestation, on the other hand, allows users to verify the integrity of a remote CVM (or enclave) running in the cloud before transmitting any sensitive data. Originally exclusive to CPUs, confidential computing is now supported by the latest GPUs as well, such as the NVIDIA H100 [27]. Many cloud providers offer confidential computing as a service, primarily through the use of CVMs [14]. Unlike regular VMs, which can share memory for read-only data such as LLM weights, CVMs do not share memory, to ensure that confidential data remains securely isolated and encrypted. In this work, we use the terms TEE and CVM interchangeably.

2.2.2. Confidential Inferencing. A straightforward approach to applying confidential computing to the LLM service is to serve multiple users with a single LLM instance running within a shared CVM (Figure 2b). This method is used by most existing commercial services, such as confidential inferencing in Azure [14] and AWS [15]. Although this approach effectively protects against potential threats from malicious cloud providers and adversaries that can compromise the cloud, it requires all users to fully trust the LLM provider and the CVM owner, which is not aligned with our threat model (§3.2). An alternative approach is to instantiate a separate LLM instance within a CVM for each user (Figure 2c). This setup offers stronger security, as each user is the owner of their associated CVM, making it preferable in scenarios with only a few users, as discussed in §8. However, this approach suffers from two significant inefficiencies: (1) limited scalability, as the number of concurrent user CVMs is constrained, and (2) low throughput and high latency due to reduced batch parallelism. For example, a 13B-parameter LLM requires about 27 GB of memory for its weights using 16-bit floating point, which means that a 80 GB GPU can only support up to three concurrent user CVMs. Moreover, inference is performed independently for each user, e.g., X_1W, \dots, X_nW , which is less efficient than batching as $(X_1 : \dots : X_n)W$. Our solution, SMD, addresses both challenges by isolating only the user prompt within the CVMs

while sharing the LLM among multiple users (Figure 2d).

2.3. Confidentiality without Encryption

In an information-theoretic sense, a message is secure if an eavesdropper can do no better than guessing randomly to determine its content [28], [29]. Modern encryption achieves this by transforming messages into ciphertexts that are indistinguishable from random noise. However, encryption is not the only method for ensuring message confidentiality. In this section, we first introduce the concept of *chaffing and winnowing* [30], [31] as an alternative approach to secure message confidentiality, and then present our security model for formal analysis in the following sections.

2.3.1. Chaffing and Winnowing. In native *chaffing and winnowing*, a sender secures sensitive messages by mixing them with fake ones, known as *chaffing*. For example, to secure the message “Meet at 5pm”, the sender might transmit it along with variations like “Meet at X pm”, where X ranges from 1 to 12. Assuming both the sender and the receiver share a symmetric secret key for signing and verifying the message authentication code (MAC) carried with message, the receiver can authenticate whether a message originates from the sender. Instead of appending an authentic MAC with a fake message, the sender includes a fake MAC with each fake message. This enables the receiver to identify and discard fake messages, known as *winnowing*.

The premise of confidentiality without encryption in the above protocol is that (1) an eavesdropper cannot distinguish between authentic and fake messages based on their content, while (2) the receiver can. This is achieved by (1) generating fake messages (and corresponding fake MACs) that appear authentic, and (2) using a shared symmetric secret key to differentiate the authentic MAC from the faked ones.

2.3.2. Security Model. The *chaffing and winnowing* concept described above achieves a certain level of confidentiality without encryption. However, naively applying such technique to messages in natural language is not information-theoretically secure because the distribution of the generated messages may not be uniform. The key challenges are how to *generate fake messages that appear authentic* and how to *quantify their “authenticity”*. For example, in the phrase “I am a teenager. I am X years old.”, a poorly designed *chaffing* might consider X to be any positive integer to maintain the grammatical correctness. However, a more effective *chaffing* should realize that X is most likely between 13 and 19, and it would be highly improbable for X to exceed 30, given the context of “teenager”.

To quantify the “authenticity” of fake messages, we introduce the concept of ϵ -close over a distribution \mathcal{D} to bound the “distance” between two sets of messages:

Definition 2.1 (ϵ -close over \mathcal{D}). Two sets of messages S and S' are ϵ -close over \mathcal{D} if $\max_{s \in S, s' \in S'} |P_{\mathcal{D}}(s) - P_{\mathcal{D}}(s')| < \epsilon$, where $P_{\mathcal{D}}(s)$ represents the probability of a message s as modeled by the distribution \mathcal{D} .

In this paper, unless otherwise specified, \mathcal{D} refers to the true probability distribution of messages, which is inaccessible to anyone. A language model LM can approximate \mathcal{D} , denoted as \mathcal{D}_{LM} . We define the “distance” between two distributions over a set of messages U as

$$\Delta_U(\mathcal{D}, \mathcal{D}_{LM}) = \max_{s \in U} |P_{\mathcal{D}}(s) - P_{\mathcal{D}_{LM}}(s)|.$$

If $\Delta_U(\mathcal{D}, \mathcal{D}_{LM})$ is close to zero, we say the language model LM provides a sufficiently accurate approximation of \mathcal{D} over the subdomain U .

Intuitively, if there are λ fake messages that are ϵ -close to the authentic message over \mathcal{D} and ϵ is small, these fake messages appear authentic, as their probabilities are close to that of the authentic message, bounded by ϵ . In the case that ϵ closes to zero, the distribution across these $\lambda + 1$ messages will be nearly uniform. In other words, even if an adversary obtains the plaintext of these $\lambda + 1$ messages, they can only guess randomly, with a probability of approximately $\frac{1}{\lambda+1}$ of being correct, and an advantage bounded by ϵ . However, since \mathcal{D} is inaccessible, we approximate it with \mathcal{D}_{LM} and assume that this approximation is sufficiently accurate. In §5.3, we provide a formal analysis showing that the total error is bounded by both ϵ and $\Delta_U(\mathcal{D}, \mathcal{D}_{LM})$, where U represents the union of the authentic and fake message sets.

We note that both ϵ and λ are key security factors. Our design of *prompt obfuscation* allows users to configure the desired values for these security factors, that is, ϵ_0 and λ_{min} . If fewer than λ_{min} qualified candidates that are ϵ_0 -close (e.g., λ is less than 8 in the example of “I am a teenager. I am X years old.”), *prompt obfuscation* will alert the user to a possible information leak. Details can be found in §5.

2.4. Related Work

We provide a brief overview of the existing literature on privacy-preserving LLM inference, particularly in the context of protecting information in prompts. Beyond the CVM-based solutions presented in §2.2 and Figure 2, research in this area has predominantly focused on three main approaches: differential privacy (DP), multiparty computation (MPC), and homomorphic encryption (HE).

Several studies have applied the DP principles to in-context learning by injecting noise into token distributions, generating few-shot random examples, or tuning prompts [5], [6], [32], [33]. However, these DP-based methods are task-specific (i.e., applicable only for group-level information) and compromise output invariance. Although our approach shares the DP objective of preventing observers from inferring individual user information from the overall output, SMD and PO are lossless, maintaining output invariance.

MPC has been widely applied to protect input privacy in DNN inference, and its use in LLM inference has been explored, such as using MPC-based matmul or offloading some Transformer layers [9], [34]. Despite its popularity, existing MPC methods compromise model confidentiality and are vulnerable to reconstruction attacks. HE, often combined with MPC to provide end-to-end privacy guarantees, has also been applied to DNN inference [10], [35] and,

more recently, to LLM [36], [37]. However, these methods remain impractical for widespread use, not only due to their significant computational overhead but also limitations in supporting nonlinear computations. As a result, nonlinear functions are often replaced with polynomial approximations, which impedes the use of existing well-trained models and reduces accuracy compared to state-of-the-art models.

A more recent approach focuses on privacy-preserving prompt engineering [7], [38], which anonymizes sensitive information in prompts by substituting sensitive segments with labels or alternative tokens before providing the entire prompt to the LLM. This approach shares similarities with our prompt obfuscation design, as both involve replacing segments in prompts. However, anonymization in this approach alters the output and reduces accuracy. In contrast, OSMD not only ensures output invariance, but also adds an additional layer of protection by retaining the entire prompt (excluding public segments such as system messages) and the private KV cache within the CVM. To the best of our knowledge, OSMD is the first scalable design that applies confidential computing to LLM serving without trusting the LLM itself.

3. Design Overview

In this section, we introduce the design goals of Confidential Prompting (§3.1), its threat model (§3.2), and the overview of OSMD (§3.3).

3.1. Design Space

In addition to the primary goal of securing users’ prompts in cloud-hosted LLM serving, we consider several constraints and trade-offs in the design of Confidential Prompting.

Constraints Our design respects three key constraints:

- Output invariance: Protection measures must not change the output of the cloud LLM. We believe output invariance is crucial, particularly for tasks such as summarizing clinical notes, where even a small accuracy error could lead to serious consequences for users’ health.
- Model confidentiality: Users must not know the weights of the cloud LLM. This is critical because the LLM’s weights constitute an intellectual property of the cloud LLM provider. Preserving model confidentiality enhances Confidential Prompting’s deployability in real-world.
- Compute efficiency: Protection measures must not significantly increase the cost of the service. Although security is not free, we believe that a more affordable solution will be more attractive to users.

Trade-offs We make two important trade-offs in designing Confidential Prompting. First, although it is desirable to achieve prompt confidentiality and compute efficiency simultaneously, when faced with a choice, we prioritize confidentiality over efficiency, since protecting prompt confidentiality is our main objective. Second, we strike a balance between scalability in terms of the number of users and throughput of the prompting for an individual user. Although

it is preferable to maximize both, when we have to choose one over the other, we prioritize scalability, as cloud LLMs typically serve a large number of users.

3.2. Threat Model

3.2.1. Trusted Computing Base (TCB). We assume that the users’ local machines and the cloud’s computing hardware, such as CPUs and GPUs, are trustworthy. Particularly we trust the hardware’s architectural extensions related to confidential computing, such as Intel TDX [26], AMD SEV [25] and Nvidia GPU CC [27]. This means that users can verify the integrity of their own Confidential Virtual Machines (CVMs) running in the cloud and once verified, these CVMs are trusted. Consequently, we treat a user and its CVM as the same party, even though the CVMs are hosted in the cloud.

We assume that the communication channels from users to their CVMs are secure, for example, encrypted with TLS. On the other hand, because CVMs are hosted in the cloud, the cloud vendor can control the outbound network bandwidth allocated to the CVMs, and even inspect the outbound data. This bandwidth management and inspection are crucial to maintaining model confidentiality while allowing the CVMs to read the LLM weights.

Finally, we assume the users and their CVMs privately share the key (or called seed) for a pseudorandom function.

3.2.2. Threat Model. We adopt the Honest-but-Curious (HBC) adversary model with respect to cloud LLM providers. In this model, the cloud LLM provider faithfully follows the prescribed computation steps for LLM inference, but seeks to extract as much information as possible from users. Specifically, we assume that the cloud LLM provider has access to the tokens generated during the decoding phase and their associated public KV attention states. In contrast, user prompts and the associated private KV attention states remain securely within the CVMs, inaccessible to the cloud LLM provider (Figure 2d). However, the cloud LLM provider may attempt reconstruction attacks to retrieve sensitive information stored in the CVMs, leveraging the known public states and its observation of the interactions between the LLM and the CVMs.

We do not consider attacks that can compromise the CVMs, the communication channels, or the pseudorandom function (PRF). Denial of service (DoS) attacks are also out of scope in this work. We note that confidential computing systems generally assume stronger threat models than HBC. Confidential Prompting requires a weaker threat model as it offloads most computations outside of the CVM for efficiency, but does not check the integrity of their results. We discuss possible strategies for a stronger threat model in §8.

3.3. OSMD Overview

The objective of Confidential Prompting is to protect the user’s input, or prompts, when interacting with the cloud LLM. OSMD’s core design components, *Secure Multi-party Decoding (SMD)* and *Prompt Obfuscation (PO)*, are designed

to satisfy all the constraints outlined in §3.1. Figure 1 illustrates how SMD and PO work together to defend against the threat model described in §3.2. We next provide a detailed explanation of the collaboration between SMD and PO.

Initialization The user first initializes a CVM in the cloud and verifies its integrity through remote attestation (§2.2). Next, the user tags the sensitive portions of their prompt, encrypts it locally, and transmits the encrypted prompt to the CVM. Assuming that the user and the CVM share symmetric secret keys for a secure channel, the CVM can exclusively decrypt and parse the encrypted prompt. In particular, tagging sensitive portions can be automated using tools such as Google’s PII detection tool, as demonstrated in our prototype §7.1 and discussed in §8.

Prefill and Prompt Obfuscation (§4.1 and §5) For each tagged sensitive subsequence S_{target} in the prompt S , the CVM samples a set of fake n-grams S_{fake} (§5.1), such that for each $C \in S_{fake}$,

$$\|P(C|S - S_{target}) - P(S_{target}|S - S_{target})\| < \epsilon$$

where ϵ is an error bound parameter close to 0, and the operation $S_a - S_b$ returns the result of removing subsequence S_b from S_a . The CVM generates λ *virtual prompts* using S_{fake} and generates idx with a pseudorandom function (PRF), which serves as the index of the authentic prompt among the $\lambda + 1$ prompts. Finally, the CVM computes the *private KV cache* for all $\lambda + 1$ prompts.

As its name suggests, virtual prompts are “virtual”. Instead of computing the KV cache for each of the λ virtual prompts individually, the CVM uses a memory efficient approach to jointly store them (§5.2). Additionally, allowing the CVM to access the LLM’s weights during the prefill phase does not compromise the *model confidentiality* constraint, as discussed in §3.2 and §4.1.

Secure Multi-party Decoding (§4.2) SMD decouples the attention computation in the decoding phase into a two-party computation. One party, the CVM, has exclusive access to the user prompts and maintains the private KV cache within the CVM. SMD enables scalable use of CVMs, as the CVMs do not require access to LLM weights after the prefill phase, addressing the *compute efficiency* challenges of applying CVMs to the LLM service. Furthermore, SMD is lossless, ensuring that it meets the *output invariance* constraint.

Although SMD is vulnerable to reconstruction attacks, PO mitigates this issue at the cost of redundant decoding and communication. After generating output tokens, the CVM sends the responses for all $\lambda + 1$ prompts back to the user. It is worth noting that the user already knows the value of the index idx , because we assume the user and the CVM share the key (or called seed) of the PRF (§3.2). This allows the user to perform *winnowing* and extract the authentic response.

Offloading Sampling to User As a variant of the Prompt Obfuscation described above, users may choose to offload the fake n-gram sampling to their local devices. Our sampling algorithm (Algorithm 1) requires a language model LM to

approximate the authentic language distribution \mathcal{D} . Sampling in the CVM can leverage either the cloud LLM or a small language model (SLM) hosted within the CVM, although the latter may increase the CVM size. In contrast, offloading is practical and beneficial because: (1) According to our analysis in §5.3, the security of PO depends on the distance $\Delta_U(\mathcal{D}, \mathcal{D}_{LM})$, which is independent of whether the model used is a powerful cloud LLM or a less powerful SLM on the user’s device. In fact, a local SLM fine-tuned with user data may be more effective, as it can automatically detect and better anonymize sensitive information based on the user’s habits, and thus more secure than generic cloud LLMs. In practice, local models such as Apple Intelligence are gaining popularity. (2) The tagged sensitive subsequences S_{target} are usually “common” subtexts, which do not necessarily require a powerful cloud LLM for sampling replacements. (3) Offloading reduces the size of the CVM and the time to sample fake n-grams on the server side.

Further discussion of the variants of PO is provided in §8. In the following, we introduce the design details without offloading, as the modifications for the offloading scenario are straightforward.

4. Efficient Prompt Protection with Confidential Computing

The main obstacles to using CVMs for LLM serving stem from keeping LLM weights in each CVM, as discussed in §2.2. We solve this challenge by eliminating the need to store LLM weights in CVMs after the initial prefill operation. Our key insight is that the decoding operation in LLMs can be formulated as a secure multi-party computation, where only one party needs to access the LLM weights. Specifically, we distinguish K, V attention states into *private* and *public* parts. The user prompt’s K, V states are private and are kept confidential in the CVM, while the generated sequence’s K, V states are public and shared with the LLM. We detail the inference protocol as follows.

We define three participants: (1) *Alice*, the user; (2) *Eve*, the cloud LLM provider; and (3) *Ted*, Alice’s CVM instance running on Eve’s premises. As mentioned in §3.2, we treat Alice and Ted as one party, assuming their communication is secure, while Eve follows the protocol, but tries to extract the maximum information from Ted.

- 1) **Prefill**(§4.1): Alice sends a prompt to Ted. Ted computes (K_{Pvt}, V_{Pvt}) states for the prompt and generates the first token. Ted sends the first token to Eve.
- 2) **Decoding** (§4.2): For each transformer layer, Eve computes $Q_{New}, K_{New}, V_{New}$ of the received token, appends K_{New}, V_{New} to K_{Pub}, V_{Pub} , and shares Q_{New} with Ted. Ted responds with $\sigma(Q_{New} K_{Pvt}^\top) V_{Pvt}$. Eve computes $\sigma(Q_{New} K_{Pub}^\top) V_{Pub}$ and recovers $\sigma(Q_{New} K^\top) V$ using Theorem 4.1. If it is the final layer, the output Y is sent to Ted.
- 3) Ted samples a new token from Y and sends it to Eve and Alice. Go to Step 2 until [EOS].

This protocol can be generalized to scenarios with multiple users, each with their own CVM operating in the cloud.

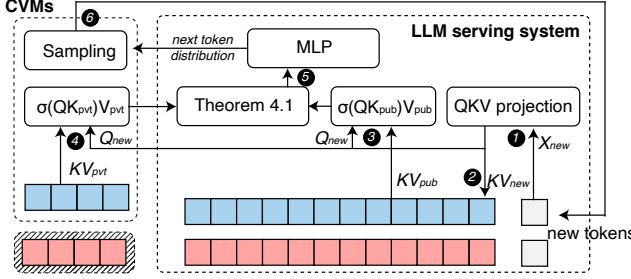


Figure 3: **SMD overview** on a simplified Transformer layer. ① Project hidden state X of a new input token to $Q_{\text{new}}, K_{\text{new}}, V_{\text{new}}$. ② Add $K_{\text{new}}, V_{\text{new}}$ to the public KV cache. ③ compute public attention (batch-process all users), ④ compute private attention in each user’s CVM, ⑤ combine results for final attention output. The next token distributions are returned to user CVMs to sample and repeat the process.

4.1. Prefill in CVM

Upon receiving Alice’s n -token prompt, Ted computes the attention states $K_{\text{Pvt}} \in \mathbb{R}^{n \times d}$ and $V_{\text{Pvt}} \in \mathbb{R}^{n \times d}$, and sends the first token to Eve. The LLM weights are discarded after prefill. We introduce two optimizations. (i) Since LLM weights are used only once, we employ a memory-efficient strategy where Ted fetches the weights as needed and discards them after use, limiting memory usage to a single layer. (ii) Not all portions of the user prompt are sensitive; for instance, common system messages can be public. Users can designate sensitive parts of the prompt using the `<confidential/>` tag. Ted stores K_{Pvt} and V_{Pvt} only for the sensitive parts, migrating the rest to K_{Pub} and V_{Pub} on Eve.

Security analysis of model confidentiality Ted requires read-only access to Eve’s LLM weights in the prefill phase. As assumed in §3.2, Eve can inspect Ted’s outbound data to prevent weight leakage to Alice. Eve is able to check the integrity of the outbound data because Eve knows the LLM responses and the responses are not encrypted. We note that even the use of PO (§5) does not require Ted to send Alice the value of the index of the authentic response among the $\lambda + 1$ candidates, which would create a side channel for the leakage of LLM weights. This is because Alice shares the key (or called seed) of the PRF with Ted(§3.2) and, as a result, already knows the index.

4.2. Secure Multi-party Decoding (SMD)

We formulate the decoding operation as a secure two-party computation based on the online softmax calculation [39], allowing Eve to retrieve the full attention output without knowing K_{Pvt} and V_{Pvt} . Specifically, we introduce the following theorem for two-party decoding:

Theorem 4.1 (Two-party attention computation). *Let $K = \text{concat}(K_{\text{Pvt}}, K_{\text{Pub}}) \in \mathbb{R}^{n \times d}$, $V = \text{concat}(V_{\text{Pvt}}, V_{\text{Pub}}) \in$*

$\mathbb{R}^{n \times d}$, $Q \in \mathbb{R}^d$, and σ be a softmax function. Then,

$$\begin{aligned} \sigma(QK^\top)V &= \frac{\gamma_{\text{Pvt}}}{\gamma_{\text{Pvt}} + \gamma_{\text{Pub}}} \sigma(QK_{\text{Pvt}}^\top)V_{\text{Pvt}} \\ &\quad + \frac{\gamma_{\text{Pub}}}{\gamma_{\text{Pvt}} + \gamma_{\text{Pub}}} \sigma(QK_{\text{Pub}}^\top)V_{\text{Pub}} \end{aligned} \quad (1)$$

where $\gamma_{\text{Pvt}}, \gamma_{\text{Pub}}$ are denominators of each softmax operation, e.g. $\gamma_{\text{Pvt}} = \sum \exp(QK_{\text{Pvt}}^\top)$.

Theorem 4.1 is lossless and its proof is available in the appendix. This theorem serves as the foundation for the design of SMD, which offers two key benefits. First, Eve can batch process all public states $(Q, K_{\text{Pub}}, V_{\text{Pub}})$ of different users in parallel using a single set of LLM weights. Second, computations in Ted have a fixed cost and do not involve LLM weights, allowing Ted to retain only a small amount of memory for the private states. In addition, SMD only induces a constant communication overhead of $2d+1$ floating points in each round. We note that computing γ_{Pvt} and γ_{Pub} individually is numerically unstable due to its exponential term. Instead, we compute $\gamma_{\text{Pvt}} = \sum \exp(QK_{\text{Pvt}}^\top - m_{\text{Pvt}})$, where $m_{\text{Pvt}} = \max(QK_{\text{Pvt}}^\top)$. The coefficients in Theorem 4.1 become $\frac{\gamma_{\text{Pvt}}}{\gamma_{\text{Pvt}} + \alpha\gamma_{\text{Pub}}}$ and $\frac{\gamma_{\text{Pub}}}{\alpha^{-1}\gamma_{\text{Pvt}} + \gamma_{\text{Pub}}}$, where $\alpha = \exp(m_{\text{Pub}} - m_{\text{Pvt}})$.

4.3. Security Analysis

Under the assumptions outlined in §3.2, Alice’s prompt remains secure both during transmission to Ted and throughout the prefill phase within the CVM. During the decoding phase, Ted ensures that neither the prompt nor the private KV cache is exposed to Eve. In other words, maintaining the private KV cache within the CVM ensures prompt confidentiality. Even if Eve disregards the private KV cache stored in the CVM and attempts to recompute the KV attention states, she is unable to do so because the prompt itself remains secure within the CVM as well. Instead, Eve only has access to the generated tokens and the output of $\sigma(Q_{\text{New}}K_{\text{Pvt}}^\top)V_{\text{Pvt}}$ from Ted, which can not be directly reversed to retrieve the prompt or private KV attention states.

This security analysis suggests that Eve has the only opportunity to extract the private user prompt (or the embedding of the prompt $X_{\text{Pvt}} \in \mathbb{R}^{n_{\text{Pvt}} \times d}$, where $K_{\text{Pvt}} = X_{\text{Pvt}}W_K$ and $V_{\text{Pvt}} = X_{\text{Pvt}}W_V$) through (semi) black-box reconstruction attacks. In a simpler case, Eve can attempt to find an approximate solution \tilde{X}_{Pvt} for

$$\| \text{Ted}(Q) - \sigma(Q(\tilde{X}_{\text{Pvt}}W_K)^T)(\tilde{X}_{\text{Pvt}}W_V) \| = 0 \quad (2)$$

where $\text{Ted}(Q)$ is the response from Ted. Eve can also perform a stronger reconstruction attack using public KV attention states of the generated tokens:

$$\begin{aligned} \| \text{Eve}(Q) - \sigma(Q \times \text{concat}(\tilde{X}_{\text{Pvt}}W_K, K_{\text{Pub}})^T) \\ \times \text{concat}(\tilde{X}_{\text{Pvt}}W_V, V_{\text{Pub}}) \| = 0 \end{aligned} \quad (3)$$

where $\text{Eve}(Q)$ is the result from Equation 1. Reconstruction attacks generally require a large number of observations to be effective. However, because of the autoregressive nature of LLMs, they can theoretically generate outputs of unlimited

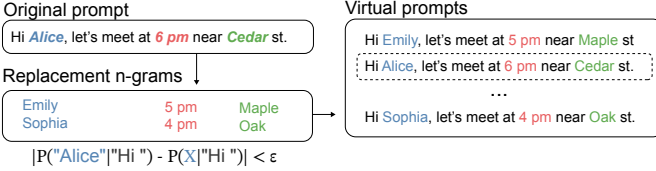


Figure 4: **PO example.** Given a prompt with its PII tagged (e.g., name and address), PO samples replacement tokens for each tagged token sequence using GQS. The generated fake tokens are statistically close to the original ones.

length, resulting in an unlimited number of public states. Although relying solely on SMD could secure the user prompt against typical adversaries who might compromise the cloud, it leaves the system vulnerable to adversaries with unlimited memory and computational resources.

5. Prompt Obfuscation

We present *prompt obfuscation (PO)*, a novel defense against reconstruction attacks. Inspired by *chaffing and winnowing* [30], [31], PO aims to fundamentally limit Eve’s ability to accurately observe Alice’s prompts, at the cost of generating redundant tokens. As mentioned in §2.3.1, the premise of confidentiality without encryption in Rivest’s work is that (1) an eavesdropper cannot distinguish between authentic and fake messages based on their content, while (2) the receiver can. PO achieves (1) by leveraging LLMs’ ability to perform infilling and (2) by exploiting the protocol’s reflective nature, in which Ted sends intermediate data to Eve for processing and the output is reflected back to Ted. During the prefill phase in the CVM (§4.1), Ted creates a set of *virtual prompts* by replacing segments of the authentic user prompt with sampled fake n-grams. In the decoding phase (§4.2), Ted instructs Eve to decode all virtual prompts and the authentic prompt in parallel, while keeping track of the authentic prompt’s index to relay the authentic output back to Alice. Figure 4 provides an example of PO.

5.1. Sampling Virtual Prompts

We introduce Greedy Quantized Sampling (GQS), a simple algorithm designed to sample fake n-grams based on the user’s prompt S , as illustrated in Algorithm 1. We ask users to mark sensitive subsequences in the prompts with `<redacted/>` tags. For simplicity, we assume that the sensitive subsequences within a prompt are independent and process them separately, denoted S_{target} . The target subsequence S_{target} may represent a name, location, medical condition, or other sensitive information. The goal of GQS is to generate multiple fake replacement subsequences that appear as authentic as the original S_{target} . In addition to S and S_{target} , GQS requires parameters ϵ and λ_{max} , as well as a pre-trained language model LM . For brevity, we denote the algorithm as $GQS(S, S_{target}, \epsilon)$.

Algorithm 1 leverages the ability of LLMs to infill missing subsequence in a prompt, that is, replacing S_{target}

with S . Some LLMs are specifically trained for infilling tasks [40], [41], [42]. It has also been shown that simple autoregressive LLMs can perform infilling when the prompts are appropriately formatted [43], such as using the *Format* function to obtain the formatted prompt \tilde{S} in Algorithm 1. Sequences $\{F_i\}$ refer to predefined control sequences used to format the prompt for the infilling task, which are determined by the chosen language model LM . For example, tokens like `<prefix>` and `<suffix>` are commonly used in fill-in-the-middle (FIM) models [44].

There are two key parameters in GQS that control the number of fake n-grams to generate: $0 < \epsilon \leq 1$ and $\lambda_{max} \in \mathbb{N}$. ϵ is the error bound for the fake n-grams, while λ_{max} controls the maximum number of candidates to consider at each step. These parameters can be adjusted according to security requirements and Ted’s available memory. Given the prompt S and the target subsequence S_{target} from Alice, Ted samples fake n-grams S_{fake} using $GQS(S, S_{target}, \epsilon)$ and constructs a set of virtual prompts by replacing S_{target} with each $C \in S_{fake}$. Alice may also provide an additional parameter, λ_{min} . If fewer than λ_{min} virtual prompts are generated, Ted will stop in the prefill phase and alert Alice to a potential information leak if the process continues.

In the case where multiple sensitive subsequences are marked with `<redacted/>` tags in a prompt, since conditioning the fake n-grams on all subsequences simultaneously is impractical due to the exponential growth in the number of candidates, we treat each selected subsequence as an independent variable. Fake n-grams are sampled for each subsequence in parallel using GQS. Under the assumption of independence, the upper bound of ϵ of the generated virtual prompts is equal to the sum of the values ϵ_i for each i -th subsequence.

5.2. Compact Representation of Virtual Prompts

We introduce a memory-efficient approach to store virtual prompts within CVMs. This approach significantly reduces memory overhead while introducing a small approximation error to the decoding of virtual prompts. It does not affect the final accuracy, as the decoding of the authentic prompt remains unaffected, and the virtual ones are eventually discarded.

Given λ virtual prompts, instead of storing all K_{Pvt} and V_{Pvt} for each virtual prompt, which would require memory proportional to $\lambda|S|$, we compute the attention states for the shared part $S - S_{target}$ separately, and share them across all virtual prompts, but not for the authentic prompt. This allows Ted to store attention states only for the individual fake n-grams $C \in S_{fake}$, reducing the memory cost to store all virtual prompts from $\lambda|S|$ to $|S - S_{target}| + \lambda|S_{target}|$.

This method introduces a small approximation error for the decoding of virtual prompts due to the attention masking effect, since the attention states for the shared $S - S_{target}$ are computed without the fake replacement $C \in S_{fake}$. However, this optimization does not affect the final accuracy, as the authentic prompt is correctly decoded.

Algorithm 1 Greedy Quantized Sampling (GQS) for Prompt Obfuscation

Require: User’s prompt S as token sequence, target subsequence S_{target} , parameters ϵ and λ_{\max} . LM is a pre-trained language model, and $\{F_i\}$ are the associated pre-defined control sequences to format the prompt. The $+$ operator indicates concatenation, while $S_a - S_b$ indicates removing subsequence S_b from S_a .

```

1:  $S_{\text{context}} \leftarrow S - S_{\text{target}}$ 
2:  $n \leftarrow |S_{\text{target}}|$ 
3:  $\tilde{S} \leftarrow \text{Format}(\{F_i\}, S_{\text{context}}, n)$  ▷ Format  $S$  for the infilling task.
4:  $\epsilon' \leftarrow \epsilon/n$ 
5:  $S_{\text{fake}} \leftarrow \{\}$ 
6: for  $i \leftarrow 1$  to  $n$  do
7:    $S_{\text{new}} \leftarrow \{\}$ 
8:    $X_{\text{ref}} \sim \text{LM}(\tilde{S} + S_{\text{target}}^{1 \dots i-1})$  ▷ LM models the distribution of the next token.
9:    $\rho \leftarrow P(X_{\text{ref}} = S_{\text{target}}^i)$  ▷ Compute the reference probability  $\rho$ 
10:  for each  $C \in S_{\text{fake}}$  do ▷ Find all tokens with probability within the same quantized bin as  $\rho$ .
11:     $X \sim \text{LM}(\tilde{S} + C)$  ▷ Each “bin” has a width of  $\epsilon'$ . There are  $\lceil \frac{1}{\epsilon'} \rceil$  bins in total.
12:     $S_{\text{new}} \leftarrow S_{\text{new}} \cup \{C + x \mid \lfloor \frac{\rho}{\epsilon'} \rfloor \cdot \epsilon' < P(X = x) \leq (\lfloor \frac{\rho}{\epsilon'} \rfloor + 1) \cdot \epsilon'\}$ 
13:  end for
14:   $S_{\text{fake}} \leftarrow \text{top-}\lambda_{\max}(S_{\text{new}})$  ▷ Only select  $\lambda_{\max}$  candidates to keep the compute cost static.
15: end for
16: return  $S_{\text{fake}}$ 

```

5.3. Security Analysis

PO adds an extra layer of protection to SMD (§4), defending against (semi) black-box reconstruction attacks in two folds. (1) First, it linearly increases the cost of reconstruction attacks, while incurring only sublinear resource usage within the CVM (§5.2) and minimal performance degradation (§7.2). (2) Second, even in the worst case where an adversary reconstructs all $\lambda + 1$ prompts (with λ being the number of virtual prompts), the adversary’s probability of correctly guessing the authentic prompt S improves by only ϵ beyond randomly guessing from the $\lambda + 1$ possible prompts, assuming that the language model LM accurately captures the true distribution \mathcal{D} . We next analyze (2) in more detail.

Theorem 5.1. *Given a user prompt S and a subsequence S_{target} , let $S_{\text{fake}} = GQS(S, S_{\text{target}}, \epsilon)$ and $\Delta = \Delta_U(\mathcal{D}, \mathcal{D}_{\text{LM}})$, where $U = \{S_{\text{target}}\} \cup S_{\text{fake}}$. Then $\{S_{\text{target}}\}$ and S_{fake} are $(\epsilon + 2\Delta)$ -close over \mathcal{D} .*

Theorem 5.1 implies that if both ϵ and Δ are small, the virtual prompts generated as described in §5.1 would appear as authentic as the user prompt S . More precisely, the maximum difference between the probabilities of any pair of authentic and fake subsequences is $\epsilon + 2\Delta$, given S as context. The proof is provided in the appendix. Suppose that we have an authentic prompt S and a set of virtual prompts $S_1, S_2, \dots, S_\lambda$. Let \mathcal{D}_{LM} be the distribution of all possible sequences modeled by LM . Theorem 5.1 essentially states that an adversary with knowledge of \mathcal{D} can guess the authentic prompt S with a probability $\epsilon + 2\Delta$ better than randomly choosing from $\lambda + 1$ possible prompts. Therefore, the security of PO can be characterized by three factors: (1) the set size, λ ; (2) the error bound of sampling, ϵ ; and (3) the gap between the true distribution and its approximation, $\Delta = \Delta_U(\mathcal{D}, \mathcal{D}_{\text{LM}})$.

In some cases, \mathcal{D} can be well captured by \mathcal{D}_{LM} . A clear example is when the number of alternative prompts is finite

and enumerable, such as “I live in [CITY]” and “I am [AGE] years old”. In such cases, PO satisfies the definition of confidentiality with a reasonably small ϵ and a large λ . Empirical evaluation results are provided in §7.1.

However, PO does not fully guarantee confidentiality when the true distribution \mathcal{D} differs from \mathcal{D}_{LM} . This can happen when \mathcal{D}_{LM} is simply not sufficiently sophisticated. In such cases, PO serves as an *obfuscation*, as its name suggests, increases the cost of cryptanalysis, but does not fully prevent it. Furthermore, the above analysis suggests that an adversary with greater knowledge of the true distribution \mathcal{D} gains an advantage in guessing. However, it is important to note that \mathcal{D} is not always accessible to adversaries, meaning that the actual error bound in practice is likely smaller than our theoretical analysis.

Another scenario in which PO does not provide full confidentiality is when the prompt S is unique. In such cases, it may be impossible to generate fake n-grams without using a large ϵ or small λ , regardless of whether \mathcal{D} is well captured by \mathcal{D}_{LM} or not. To prevent a potential information leak, PO allows users to configure the desired ϵ and λ_{\min} . If $\lambda < \lambda_{\min}$, Ted will stop in the prefill phase and alert Alice.

Finally, the security of PO also depends on whether an adversary can successfully guess the index of the authentic prompt among $\lambda + 1$ prompts, even without reconstructing all prompts. PO employs a pseudorandom function (PRF) to generate the index. As stated in §3.2, attacks on the PRF are outside the scope of our threat model.

6. Implementation

We implement OSMD (SMD+PO) based on PyTorch and target the widely adopted Llama [19] series of open-source LLMs. We next describe a few key implementations in our prototype.

LLM Serving Server. We develop an LLM serving server based on the Transformers library [45], which assumes

that all user requests arrive simultaneously (no continuous batching), for simplicity of implementation. To support SMD, we adapted the Llama model by monkey-patching its attention module. Specifically, we modified the attention score calculation to asynchronously send the query tensor (Q in Theorem 4.1) to each user via the GLOO tensor communication backend [46]. This allows us to receive private attention scores from users while computing public attention scores in parallel. The server waits for all private scores to arrive before evaluating the final attention score.

Prompt Vault. Within each user’s CVM, operations like prefill, PO, and calculating private attention scores are managed by a client called the prompt vault. The prompt vault synchronously listens to the LLM serving server to receive the Q tensor over the GLOO backend and returns results based on Theorem 4.1.

Serving virtual prompts with sub-linear memory. We implement the compact representation mechanism for virtual prompts (§5.2) using asymmetric attention masks. For example, suppose we have two prompts—real and fake—that share a common segment S_{shared} of length a . The real token sequence’s KV cache is S_{real} , and the fake one is S_{fake} , both of length b . The naive way to store attention states is to batch them:

$$(K \quad V) = \begin{pmatrix} S_{\text{shared}} & S_{\text{real}} \\ S_{\text{shared}} & S_{\text{fake}} \end{pmatrix} \in \mathbb{R}^{2 \times 2(a+b) \times d}. \quad (4)$$

Instead, our implementation flattens the attention states to eliminate redundancies:

$$(K' \quad V') = (S_{\text{shared}} \quad S_{\text{real}} \quad S_{\text{fake}}) \in \mathbb{R}^{1 \times (a+2b) \times d}. \quad (5)$$

We use a special attention mask where 1_n and 0_n denote vectors of ones or zeros of size n :

$$M = \begin{pmatrix} 1_{\text{shared}} & 1_{\text{real}} & 0_{\text{fake}} \\ 1_{\text{shared}} & 0_{\text{real}} & 1_{\text{fake}} \end{pmatrix} \in \{0, 1\}^{2 \times (a+2b)}. \quad (6)$$

The attention formula in § 2.1 then becomes:

$$Y = \text{softmax} \left(\frac{QK'^\top}{\sqrt{d}} \right) M^\top V' \in \mathbb{R}^d. \quad (7)$$

Note that approaches like pagedattention [47] can be considered for achieving the same effect, but they are not yet fully compatible with CVMs.

7. Evaluation

Our evaluation primarily aims to address two questions:

- Does our design preserve user prompt confidentiality in practice?
- Does our design meet the compute efficiency requirement, considering that output invariance and model confidentiality for SMD and PO are trivial?

To answer the first question, we empirically examine the maximum available λ for the desired error bounds given by ϵ , which are referred to as pairs of security factors (ϵ, λ) in the following, and examine other factors that influence the sampling results. Subsequently, we evaluate the performance

of the SMD + PO method compared to two naive methods based on CVM as presented in Figure 2.

Evaluation setup. Our evaluation utilizes the Llama 2 [19] models with 7B and 13B parameters, Llama 3 [48] model with 8B parameters, and Code Llama [49] model with 34B parameters. All experiments were conducted on a cloud node equipped with an NVIDIA H100 NVL GPU with 94 GB of memory, 40 AMD EPYC Genoa processor cores, and 320 GB of system memory. Architectural security features such as AMD SEV-SNP [25] and NVIDIA GPU CC [27] are enabled for evaluation that require confidential computing. It is worth noting that our design does not require confidential computing protection for the LLM serving server. However, since computing nodes with multiple GPUs that support enabling GPU CC feature were not available at the time of writing, and because NVIDIA GPU CC feature can only be enabled or disabled entirely on a single GPU, the confidential computing overhead also applies to the LLM server in the following experiments. Consequently, the performance overhead presented in this section is higher than the ideal case described in our design.

7.1. Security of Prompt Obfuscation

As discussed in §5.3, the security of Prompt Obfuscation depends on the pair of security factors (ϵ, λ) and the distance $\Delta_U(\mathcal{D}, \mathcal{D}_{\text{LM}})$. Here, \mathcal{D} represents the *true distribution* of prompts, which is inaccessible to both users and adversaries. We assume that \mathcal{D}_{LM} provides a sufficiently accurate approximation of \mathcal{D} . Based on this assumption, we empirically examine the pairs of security factors (ϵ, λ) in different categories of personally identifiable information (PII).

Dataset Preparation. We first construct the clinical dataset by combining clinical dialogues between patients and physicians [50] with clinical notes from USMLE Step 2 [51]. Additionally, we use a public resume classification dataset from Kaggle [52]. To categorize and tag the PII data, we use Google’s PII detection tool, marking each instance with a tag `<redacted>`. Details are provided in the appendix.

Exhaustive Sampling. We present the results for the examined pairs of security factors (ϵ, λ) in different categories of PII in Figure 5 and Figure 6. These value pairs are determined through an exhaustive search using the GQS algorithm (Algorithm 1) on both datasets, with Llama 3 model, $\lambda_{\text{max}} = 512$, and the sampling temperature $\tau = 0$.

Result Analysis. Our observations indicate that GQS can generate a reasonably large set of fake n-grams. For example, with $\epsilon = 0.1$, the “date” category has approximately $\lambda = 320$, which roughly corresponds to the number of days in a year, and the “age” category has $\lambda = 52$, reflecting age groups from 20 to 70. Examples of dataset samples and GQS outputs are provided in the appendix.

Effect of Different Models and Parameter Size. The impact of the model parameter size on λ is relatively small. For example, comparing Llama 2 models with 7B and 13B parameters on the clinical dataset results in only a 4%

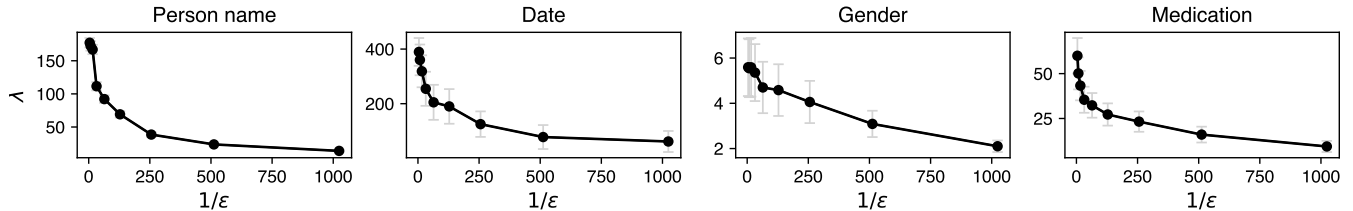


Figure 5: (ϵ, λ) pairs sampled from the clinical dataset with $\lambda_{\max} = 512$, for four selected PII categories (person name, date, gender and medication). Dots indicate the mean of λ for each ϵ , and the error bars indicate a 95% interval.

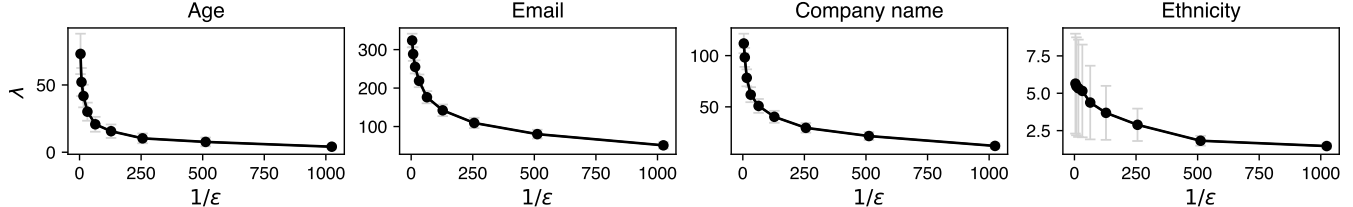


Figure 6: (ϵ, λ) pairs sampled from the resume dataset with $\lambda_{\max} = 512$, for four selected PII categories (age, email, company name and ethnicity). Dots indicate the mean of λ for each ϵ , and the error bars indicate a 95% interval.

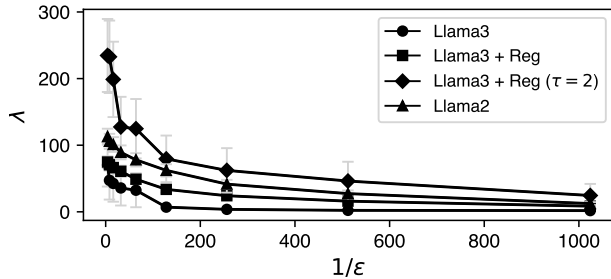


Figure 7: (ϵ, λ) pairs sampled from the clinical dataset with $\lambda_{\max} = 512$, for locational PII, e.g. address and name of places. Unless otherwise specified, the sampling temperature is set to $\tau = 1$.

difference in λ . In contrast, the choice of language model has a much more substantial effect on λ . As shown in Figure 7, there is a $2.4 \times$ difference in λ between Llama 3 and Llama 2 (13B). We observed that Llama 3, as a more advanced model than Llama 2, is more “confident” in selecting the next token, which narrows the possible candidate pool. In other words, the distribution modeled by Llama 2 is flatter, resulting in a higher λ under the same conditions.

Effect of Regularization. Grammar and typing errors in the target sequence S_{target} degrade the security of prompt obfuscation, as sequences with such errors are far less common in the distribution. Regularizing the content, such as correcting capitalization and spelling, can improve λ . We use a ChatGPT-based tool to correct typing errors in the dataset and compare the λ in Figure 7 between regularized (“Llama3+Reg”) and non-regularized (“Llama3”) datasets.

Effect of Sampling Temperature. The λ values are influenced by the token sampling temperature τ . A higher τ flattens the token distribution, increasing the number of fake n-grams that fall within the same ϵ' bin as the authentic n-gram (Algorithm 1). We present the difference in λ between $\tau = 1$

(“Llama3+Reg”) and $\tau = 2$ in Figure 7, indicating that prompt obfuscation can be more effective with a higher setting τ .

7.2. Performance Analysis

We implement two baselines for performance evaluation to demonstrate the scalability and compute efficiency of our approach: (1) *No protection*, a naive approach where every user is served with a single LLM instance within a single CVM (Figure 2b), which is intended to demonstrate the upper bound for the performance with confidential computing; and (2) *Full isolation*, a naive approach where each user is served with a dedicated LLM instance within a per-user CVM (Figure 2c). Our approach, which uses SMD (Figure 2d), is denoted as *SMD*. We compare the performance of our approach with that of *Full isolation* because the latter defends against a similar threat model as ours.

7.2.1. Scalability. Our evaluation setup includes 1 to 32 users, with prompts ranging from 64 to 256 input tokens and generating between 32 to 256 output tokens per user. We measure the average end-to-end latency for each user to receive the output tokens. Figure 8, Figure 9 and Figure 10 summarize the main results, demonstrating that our approach scales more effectively than the *Full isolation* baseline as the number of users, input/output tokens, and the model parameter size increase.

Number of Users. The primary challenge in using CVMs for LLM services is achieving scalability with a growing number of users (§2.2). *Full isolation* handle separate instances of the LLM for each user, which limits the maximum number of concurrent user CVMs due to GPU memory limitations. As shown in Figure 8, the latency of *Full isolation* increases significantly as the number of users increases. In contrast, the *SMD* approach scales effectively with the number of

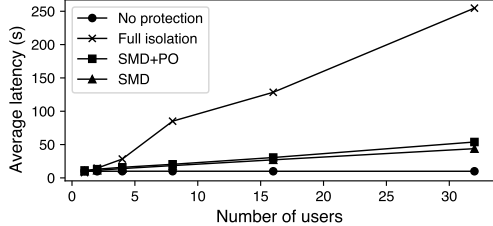


Figure 8: **Average latency with varying number of users**, served with Llama 2 (13B), 64 input tokens, 64 output tokens, and $\lambda = 8$ for the benchmark with PO.

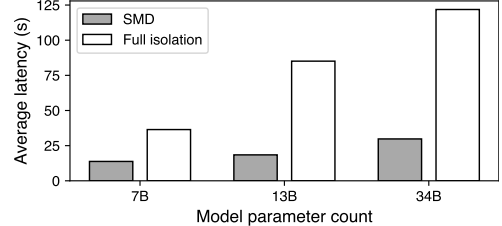


Figure 9: **Average latency with different model sizes**, measured by parameter count, with 8 users, 64 input tokens and 64 output tokens.

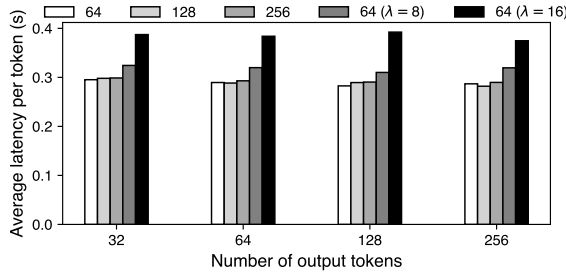


Figure 10: **Average latency in generating per output token, with varying number of input, output tokens and λ** , served with Llama 2 (13B) and for 8 users. Different groups of bars indicate different number of output tokens. The first three bars in each group indicate different input token counts while $\lambda = 0$. The other two bars in each group indicate different λ with 64 input tokens.

users, because it can host a large number of user CVMs concurrently.

Model Parameter Size. The *Full isolation* baseline also faces scalability challenges as model parameter sizes increase. In contrast, *SMD* is less affected by parameter size scaling. As presented in Figure 9, *Full isolation*’s end-to-end latency scales at a higher rate than that of *SMD* under the same conditions, when the model size increases from 7B to 34B.

Number of Input/Output Tokens. The number of input tokens primarily impacts the initial time-to-first-token (TTFT) latency. Both *Full isolation* and *SMD* experience a $15\times$ higher TTFT latency compared to the *No protection* baseline due to the absence of batch parallelism during the prefill phase. In contrast, the number of input tokens has negligible impact on the end-to-end latency in *SMD*, which reflects the time of decoding. As shown in Figure 10, the three bars in each group represent end-to-end latency for different input token counts such as 64, 128 and 256, with negligible differences among them, across different combinations of output token count and λ . Meanwhile, the increase of output token count also has negligible impact on latency per token, as decoding each token has static overhead.

7.2.2. Compute efficiency. We further analyze the overhead of *SMD* and *PO*, along with their breakdown, to demonstrate that our design is computationally efficient.

Overhead of Secure Multi-party Decoding. Secure Multi-party Decoding introduces overhead due to (1) confidential computation (CC), (2) the absence of batch processing in CVMs, and (3) communication between CVMs and the LLM. For (1), Figure 11 illustrates the impact of confidential computing (CC) on the *No protection* baseline and *SMD*. It shows that CC results in approximately 15% overhead compared to traditional computing without CC. For (2) and (3), we present *SMD*’s latency breakdown in Figure 12. The six latency sources align with the processing steps in Figure 3. The QKV projection, public attention computation and MLP are common in traditional decoding. However, the unique overhead introduced by *SMD* stems from the other three sources. Notably, the “Receiving private attention” latency includes both the time the cloud LLM spends waiting for private attention computation to finish and the communication cost. This encapsulates the overhead from (2) and (3), as either the absence of batch processing or high communication costs can cause the LLM to remain idle. As shown in Figure 12, the latency of (2) and (3) (“Sending Q_{new} ” and “Receiving private attention”) dominates the overhead, accounting for up to 40% of the total latency. In contrast, the overhead from merging attentions is relatively minor.

Overhead of Prompt Obfuscation. Prompt Obfuscation introduces overhead due to (1) sampling fake n-grams for virtual prompts, which increases TTFT, and (2) decoding for λ virtual prompts. For (1), Figure 13 illustrates the sampling latency for virtual prompts. The average sampling time for an eight-token replacement using $\lambda = 512$ and $\epsilon = 1/32$ is around 1 second. Sampling multiple subsequences can be batched, for example, 16 subsequences take about 1.5 seconds. Lower ϵ results in faster sampling due to a reduced λ . For (2), the impact of decoding virtual prompts on latency is shown in Figure 14. When $\lambda \leq 8$, the overhead is less than 3%. However, the overhead increases as λ grows: at $\lambda = 64$ and $\lambda = 128$, the overhead is approximately 7% and 30%, respectively. This overhead also scales with the number of users. As shown in Figure 10, for 8 users, the overhead of $\lambda = 8$ and $\lambda = 16$ is around 8% and 25%, respectively. Fundamentally, the overhead grows with the total number of prompts increases, as the LLM processes user prompts and virtual prompts equally. On the other hand, virtual prompts impose minimal overhead on the CVM memory footprint, thanks to our memory-efficient approach

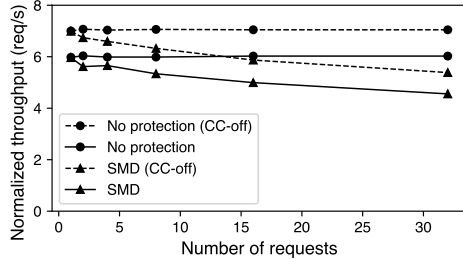


Figure 11: **Normalized throughput** with varying number of requests, 13B model, 64 input and 64 output tokens. “CC-off” indicates the throughput of conducting the benchmarks under the same condition with CC features disabled.

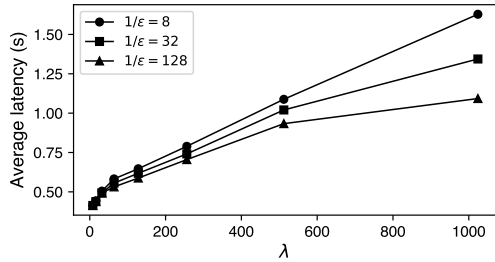


Figure 13: Average latency of sampling virtual prompts with varying λ_{\max} and ϵ for eight-token replacement in Llama 3.

for storing virtual prompts (§5.2). In conclusion, the use of Prompt Obfuscation and its associated overhead reflects a key trade-off in our design, as outlined in §3.1, that is balancing prompt confidentiality (§5.3) with compute efficiency.

8. Concluding Remarks

Cloud-based LLM services are becoming pervasive in our daily lives, but raise privacy concerns since users must submit their prompts to the cloud. OSMD combines two techniques to protect user prompts from LLM providers: secure multiparty decoding (SMD) and prompt obfuscation (PO). SMD fully leverages the confidential computing capabilities of modern hardware for efficient and scalable confidential prompting. PO, on the other hand, leverages the statistical properties of the LLM itself to achieve confidentiality without encryption. Our proposed techniques have the potential to enable privacy-preserving LLM applications such as chatbots and AI assistants that interact with a large number of end users, without high operational costs. Next, we discuss some limitations in OSMD as well as new opportunities.

When OSMD is impractical. In scenarios with only a few users but large workloads, the approach of serving entire LLM instances within per-user CVMs may be more practical. This is often the case for institutions or companies, a use case supported by several providers, such as OpenAI’s Foundry. In contrast, SMD enables efficient confidential prompting for a vast number of end users, making it ideal for services that directly interact with large audiences, such as chatbots or personal assistants.

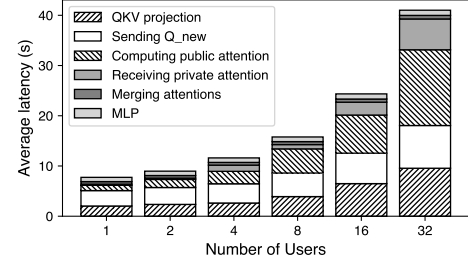


Figure 12: **Overhead breakdown of SMD** in the 13B model. As the number of users increases, the communication overhead of sending Q and receiving private attention increases linearly.

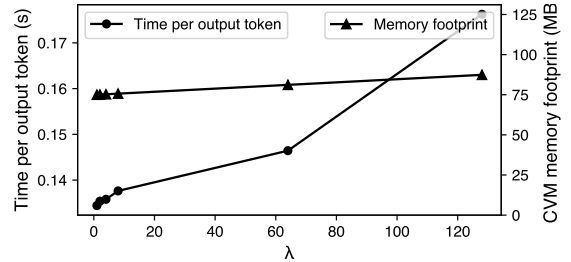


Figure 14: Average latency in generating per output token, and CVM memory footprint, with varying λ , for one user.

Integrity checks in SMD. One limitation of SMD is that it assumes a passive adversary model. This is because Ted does not check the integrity of the Q it receives. For stronger threat models that do not assume that adversaries will follow the protocol, integrity checking mechanisms on the received Q are necessary. For example, Ted can partially retain the LLM weights in the TEE and use randomized algorithms, such as Freivalds’ algorithm, to check the integrity of the received Q without fully recomputing it, or implement a zero-knowledge protocol (ZKP).

Automatic / standalone PO. Prompt obfuscation requires users to annotate the `<redacted/>` sequences. This process can be automated using a PII screening tool or a smaller local language model to identify PII. Furthermore, prompt obfuscation has the potential to be used as a standalone tool for privacy-preserving LLM inference. For instance, users can create virtual prompts using a local LLM and GQS algorithm, and then utilize them for black-box cloud LLMs (e.g., ChatGPT) to generate text, without revealing identifiable information to the cloud provider.

Acknowledgments

This work is supported in part by NSF Athena AI Institute (Award #2112562) and Yale University.

References

- [1] P. Farrell, “JPMorgan restricts ChatGPT usage for its 250K staff over fears it could steal sensitive banking secrets,” <https://www.dailymail.co.uk/news/article-11780501/JPMorgan-restricts-ChatGPT-usage-250-000-staff-data-privacy-fears.html>, 2023.
- [2] S. Ray, “Apple Joins A Growing List Of Companies Cracking Down On Use Of ChatGPT By Staffers—Here’s Why,” <https://www.forbes.com/sites/siladityaray/2023/05/19/apple-joins-a-growing-list-of-companies-cracking-down-on-use-of-chatgpt-by-staffers-heres-why/?sh=49380e9628ff>, 2023.
- [3] EU, “General Data Protection Regulation (GDPR),” <https://gdpr-info.eu/>, 2016.
- [4] N. Lomas, “Italy orders ChatGPT blocked citing data protection concerns,” <https://techcrunch.com/2023/03/31/chatgpt-blocked-italy/>, 2023.
- [5] T. Wu, A. Panda, J. T. Wang, and P. Mittal, “Privacy-preserving in-context learning for large language models,” *arXiv preprint arXiv:2305.01639*, 2023.
- [6] X. Tang, R. Shin, H. A. Inan, A. Manoel, F. Mireshghallah, Z. Lin, S. Gopi, J. Kulkarni, and R. Sim, “Privacy-preserving in-context learning with differentially private few-shot generation,” *arXiv preprint arXiv:2309.11765*, 2023.
- [7] Y. Chen, T. Li, H. Liu, and Y. Yu, “Hide and seek (has): A lightweight framework for prompt privacy protection,” *arXiv preprint arXiv:2309.03057*, 2023.
- [8] J. Lin, J. Tang, H. Tang, S. Yang, W.-M. Chen, W.-C. Wang, G. Xiao, X. Tang, C. Gan, and S. Han, “Awq: Activation-aware weight quantization for llm compression and acceleration,” in *MLSys*, 2024.
- [9] D. Li, R. Shao, H. Wang, H. Guo, E. P. Xing, and H. Zhang, “Mpcformer: fast, performant and private transformer inference with mpc,” *arXiv preprint arXiv:2211.01452*, 2022.
- [10] Z. Huang, W.-j. Lu, C. Hong, and J. Ding, “Cheetah: Lean and fast secure two-party deep neural network inference,” in *31st USENIX Security Symposium (USENIX Security 22)*, 2022, pp. 809–826.
- [11] M. Hao, H. Li, H. Chen, P. Xing, G. Xu, and T. Zhang, “Iron: Private inference on transformers,” *Advances in neural information processing systems*, vol. 35, pp. 15 718–15 731, 2022.
- [12] C. C. C. (CCC), “The Linux Foundation Projects,” <https://confidentialcomputing.io/>, 2023.
- [13] T. Lee, Z. Lin, S. Pushp, C. Li, Y. Liu, Y. Lee, F. Xu, C. Xu, L. Zhang, and J. Song, “Occlumency: Privacy-preserving remote deep-learning inference using sgx,” in *The 25th Annual International Conference on Mobile Computing and Networking*, 2019, pp. 1–17.
- [14] M. Russinovich, “Azure AI Confidential Inferencing: Technical Deep Dive,” <https://techcommunity.microsoft.com/t5/azure-confidential-computing/azure-ai-confidential-inferencing-technical-deep-dive/ba-p/253150>, 2024.
- [15] C. Renzo, L. Aliberti, J. Miles, and J. Kovba, “Large language model inference over confidential data using AWS Nitro Enclaves,” <https://aws.amazon.com/blogs/machine-learning/large-language-model-inference-over-confidential-data-using-aws-nitro-enclaves/>, 2024.
- [16] A. Radford, J. Wu, R. Child, D. Luan, D. Amodei, I. Sutskever *et al.*, “Language models are unsupervised multitask learners,” *OpenAI blog*, vol. 1, no. 8, p. 9, 2019.
- [17] T. Brown, B. Mann, N. Ryder, M. Subbiah, J. D. Kaplan, P. Dhariwal, A. Neelakantan, P. Shyam, G. Sastry, A. Askell *et al.*, “Language models are few-shot learners,” *Advances in neural information processing systems*, vol. 33, pp. 1877–1901, 2020.
- [18] J. Achiam, S. Adler, S. Agarwal, L. Ahmad, I. Akkaya, F. L. Aleman, D. Almeida, J. Alten Schmidt, S. Altman, S. Anadkat *et al.*, “Gpt-4 technical report,” *arXiv preprint arXiv:2303.08774*, 2023.
- [19] H. Touvron, T. Lavigra, G. Izacard, X. Martinet, M.-A. Lachaux, T. Lacroix, B. Rozière, N. Goyal, E. Hambo, F. Azhar *et al.*, “Llama: Open and efficient foundation language models,” *arXiv preprint arXiv:2302.13971*, 2023.
- [20] A. Vaswani, N. Shazeer, N. Parmar, J. Uszkoreit, L. Jones, A. N. Gomez, Ł. Kaiser, and I. Polosukhin, “Attention is all you need,” *Advances in neural information processing systems*, vol. 30, 2017.
- [21] M. Ott, S. Edunov, A. Baevski, A. Fan, S. Gross, N. Ng, D. Grangier, and M. Auli, “fairseq: A fast, extensible toolkit for sequence modeling,” in *Proceedings of the 2019 Conference of the North American Chapter of the Association for Computational Linguistics: Human Language Technologies, NAACL-HLT 2019, Minneapolis, MN, USA, June 2-7, 2019, Demonstrations*, W. Ammar, A. Louis, and N. Mostafazadeh, Eds. Association for Computational Linguistics, 2019, pp. 48–53. [Online]. Available: <https://doi.org/10.18653/v1/n19-4009>
- [22] M. Shoeybi, M. Patwary, R. Puri, P. LeGresley, J. Casper, and B. Catanzaro, “Megatron-Lm: Training multi-billion parameter language models using model parallelism,” *CoRR*, vol. abs/1909.08053, 2019. [Online]. Available: <http://arxiv.org/abs/1909.08053>
- [23] R. Pope, S. Douglas, A. Chowdhery, J. Devlin, J. Bradbury, J. Heek, K. Xiao, S. Agrawal, and J. Dean, “Efficiently scaling transformer inference,” *Proceedings of Machine Learning and Systems*, vol. 5, pp. 606–624, 2023.
- [24] I. Gim, G. Chen, S.-s. Lee, N. Sarda, A. Khandelwal, and L. Zhong, “Prompt cache: Modular attention reuse for low-latency inference,” *arXiv preprint arXiv:2311.04934*, 2023.
- [25] AMD, “AMD secure encrypted virtualization (SEV),” <https://www.amd.com/en/developer/sev.html>, 2023.
- [26] Intel, “Intel trust domain extensions (Intel TDX),” <https://www.intel.com/content/www/us/en/developer/articles/technical/intel-trust-domain-extensions.html>, 2023.
- [27] Nvidia, “Nvidia confidential computing,” <https://www.nvidia.com/en-us/data-center/solutions/confidential-computing/>, 2023.
- [28] C. E. Shannon, “Communication theory of secrecy systems,” *The Bell system technical journal*, vol. 28, no. 4, pp. 656–715, 1949.
- [29] U. Maurer, “Information-theoretic cryptography,” in *Advances in Cryptology — CRYPTO ’99*, ser. Lecture Notes in Computer Science, M. Wiener, Ed., vol. 1666. Springer-Verlag, 8 1999, pp. 47–64.
- [30] R. L. Rivest, “Chaffing and winnowing: Confidentiality without encryption,” *CryptoBytes (RSA laboratories)*, vol. 4, no. 1, pp. 12–17, 1998.
- [31] M. Bellare and A. Boldyreva, “The security of chaffing and winnowing,” in *Advances in Cryptology—ASIACRYPT 2000: 6th International Conference on the Theory and Application of Cryptology and Information Security Kyoto, Japan, December 3–7, 2000 Proceedings 6*. Springer, 2000, pp. 517–530.
- [32] A. Panda, T. Wu, J. T. Wang, and P. Mittal, “Differentially private in-context learning,” *arXiv preprint arXiv:2305.01639*, 2023.
- [33] J. Hong, J. T. Wang, C. Zhang, Z. Li, B. Li, and Z. Wang, “Dp-opt: Make large language model your privacy-preserving prompt engineer,” *arXiv preprint arXiv:2312.03724*, 2023.
- [34] Y. Akimoto, K. Fukuchi, Y. Akimoto, and J. Sakuma, “Privformer: Privacy-preserving transformer with mpc,” in *2023 IEEE 8th European Symposium on Security and Privacy (EuroS&P)*. IEEE, 2023, pp. 392–410.
- [35] D. Rathee, M. Rathee, N. Kumar, N. Chandran, D. Gupta, A. Rastogi, and R. Sharma, “Cryptflow2: Practical 2-party secure inference,” in *Proceedings of the 2020 ACM SIGSAC Conference on Computer and Communications Security*, 2020, pp. 325–342.
- [36] X. Liu and Z. Liu, “Llms can understand encrypted prompt: Towards privacy-computing friendly transformers,” *arXiv preprint arXiv:2305.18396*, 2023.

- [37] Q. Pang, J. Zhu, H. Möllering, W. Zheng, and T. Schneider, “Bolt: Privacy-preserving, accurate and efficient inference for transformers,” in *2024 IEEE Symposium on Security and Privacy (SP)*. IEEE, 2024, pp. 4753–4771.
- [38] K. Edemacu and X. Wu, “Privacy preserving prompt engineering: A survey,” *arXiv preprint arXiv:2404.06001*, 2024.
- [39] M. Milakov and N. Gimelshein, “Online normalizer calculation for softmax,” *arXiv preprint arXiv:1805.02867*, 2018.
- [40] J. Devlin, M.-W. Chang, K. Lee, and K. Toutanova, “Bert: Pre-training of deep bidirectional transformers for language understanding,” *arXiv preprint arXiv:1810.04805*, 2018.
- [41] C. Donahue, M. Lee, and P. Liang, “Enabling language models to fill in the blanks,” *arXiv preprint arXiv:2005.05339*, 2020.
- [42] M. Bavarian, H. Jun, N. Tezak, J. Schulman, C. McLeavey, J. Tworek, and M. Chen, “Efficient training of language models to fill in the middle,” *arXiv preprint arXiv:2207.14255*, 2022.
- [43] X. Ning, Z. Lin, Z. Zhou, H. Yang, and Y. Wang, “Skeleton-of-thought: Large language models can do parallel decoding,” *arXiv preprint arXiv:2307.15337*, 2023.
- [44] R. Li, L. B. Allal, Y. Zi, N. Muennighoff, D. Kocetkov, C. Mou, M. Marone, C. Akiki, J. Li, J. Chim *et al.*, “Starcoder: may the source be with you!” *arXiv preprint arXiv:2305.06161*, 2023.
- [45] T. Wolf, L. Debut, V. Sanh, J. Chaumond, C. Delangue, A. Moi, P. Cistac, T. Rault, R. Louf, M. Funtowicz, J. Davison, S. Shleifer, P. von Platen, C. Ma, Y. Jernite, J. Plu, C. Xu, T. L. Scao, S. Gugger, M. Drame, Q. Lhoest, and A. M. Rush, “Transformers: State-of-the-art natural language processing,” in *Proceedings of the 2020 Conference on Empirical Methods in Natural Language Processing: System Demonstrations*. Online: Association for Computational Linguistics, Oct. 2020, pp. 38–45. [Online]. Available: <https://www.aclweb.org/anthology/2020.emnlp-demos.6>
- [46] Facebook, “Gloo: Collective Communications Library,” 2023, accessed: 2024-11-09. [Online]. Available: <https://github.com/facebookincubator/gloo>
- [47] W. Kwon, Z. Li, S. Zhuang, Y. Sheng, L. Zheng, C. H. Yu, J. Gonzalez, H. Zhang, and I. Stoica, “Efficient memory management for large language model serving with pagedattention,” in *Proceedings of the 29th Symposium on Operating Systems Principles*, 2023, pp. 611–626.
- [48] Meta, 2024. [Online]. Available: <https://llama.meta.com/llama3/>
- [49] ——, 2024. [Online]. Available: <https://ai.meta.com/blog/code-llama-large-language-model-coding/>
- [50] A. Ben Abacha, W.-w. Yim, Y. Fan, and T. Lin, “An empirical study of clinical note generation from doctor-patient encounters,” in *Proceedings of the 17th Conference of the European Chapter of the Association for Computational Linguistics*. Dubrovnik, Croatia: Association for Computational Linguistics, May 2023, pp. 2291–2302. [Online]. Available: <https://aclanthology.org/2023.eacl-main.168>
- [51] NBME, “Score clinical patient notes,” *Kaggle competition*, 2022. [Online]. Available: <https://www.kaggle.com/competitions/nbme-score-clinical-patient-notes>
- [52] A. Mitsu and T. Yoshihide, “Resume text classification dataset,” *Kaggle competition*, 2021. [Online]. Available: <https://www.kaggle.com/datasets/chingkuangkam/resume-text-classification-dataset>
- [53] U. HHS, “Health Insurance Portability and Accountability Act of 1996 (HIPAA),” <https://www.cdc.gov/phlp/php/resources/health-insurance-portability-and-accountability-act-of-1996-hipaa.html>, 1996.

9. Appendix

9.1. Proof of Theorem 4.1

Let $Q \in \mathbb{R}^d$ be the query vector. Partition the key and value matrices $K \in \mathbb{R}^{n \times d}$ and $V \in \mathbb{R}^{n \times d}$ into private and public components:

$$K = \begin{bmatrix} K_{\text{Pvt}} \\ K_{\text{Pub}} \end{bmatrix}, \quad V = \begin{bmatrix} V_{\text{Pvt}} \\ V_{\text{Pub}} \end{bmatrix}.$$

Compute the attention scores s by:

$$s = QK^\top = [QK_{\text{Pvt}}^\top \quad QK_{\text{Pub}}^\top] = [s_{\text{Pvt}} \quad s_{\text{Pub}}],$$

where $s_{\text{Pvt}} = QK_{\text{Pvt}}^\top$ and $s_{\text{Pub}} = QK_{\text{Pub}}^\top$. Define the softmax denominators:

$$\gamma = \sum_{i=1}^n \exp(s_i) = \gamma_{\text{Pvt}} + \gamma_{\text{Pub}},$$

with

$$\gamma_{\text{Pvt}} = \sum_{i=1}^{n_{\text{Pvt}}} \exp(s_{\text{Pvt},i}), \quad \gamma_{\text{Pub}} = \sum_{i=1}^{n_{\text{Pub}}} \exp(s_{\text{Pub},i}).$$

The attention output is:

$$\begin{aligned} \sigma(s)^\top V &= \sum_{i=1}^n \frac{\exp(s_i)}{\gamma} V_i \\ &= \frac{1}{\gamma} \left(\sum_{i=1}^{n_{\text{Pvt}}} \exp(s_{\text{Pvt},i}) V_{\text{Pvt},i} + \sum_{i=1}^{n_{\text{Pub}}} \exp(s_{\text{Pub},i}) V_{\text{Pub},i} \right) \\ &= \frac{\gamma_{\text{Pvt}}}{\gamma} \left(\frac{1}{\gamma_{\text{Pvt}}} \sum_{i=1}^{n_{\text{Pvt}}} \exp(s_{\text{Pvt},i}) V_{\text{Pvt},i} \right) \\ &\quad + \frac{\gamma_{\text{Pub}}}{\gamma} \left(\frac{1}{\gamma_{\text{Pub}}} \sum_{i=1}^{n_{\text{Pub}}} \exp(s_{\text{Pub},i}) V_{\text{Pub},i} \right) \\ &= \frac{\gamma_{\text{Pvt}}}{\gamma} (\sigma(s_{\text{Pvt}})^\top V_{\text{Pvt}}) + \frac{\gamma_{\text{Pub}}}{\gamma} (\sigma(s_{\text{Pub}})^\top V_{\text{Pub}}). \end{aligned} \quad (8)$$

Thus,

$$\begin{aligned} \sigma(QK^\top)V &= \frac{\gamma_{\text{Pvt}}}{\gamma_{\text{Pvt}} + \gamma_{\text{Pub}}} \sigma(QK_{\text{Pvt}}^\top) V_{\text{Pvt}} \\ &\quad + \frac{\gamma_{\text{Pub}}}{\gamma_{\text{Pvt}} + \gamma_{\text{Pub}}} \sigma(QK_{\text{Pub}}^\top) V_{\text{Pub}}, \end{aligned} \quad (9)$$

which completes the proof.

9.2. Proof of Theorem 5.1

To prove Theorem 5.1, we show that the two sets of subsequences are ϵ -close over \mathcal{D}_{LM} with Lemma 9.1, and $(\epsilon + 2\Delta)$ -close over \mathcal{D} .

Lemma 9.1. *Let a_1, a_2, \dots, a_n and b_1, b_2, \dots, b_n be sequences where $0 \leq a_i, b_i \leq 1$. If $|a_i - b_i| < \epsilon/n$ for all i , then $|\prod_{i=1}^n a_i - \prod_{i=1}^n b_i| < \epsilon$.*

Part I Let us denote each token in the subsequence S_{target} as random variables X_1, \dots, X_n , where X_1 is the start token and X_n is the end token. Let $f(X_i) = P(X_i | X_1, \dots, X_{i-1})$ be the conditional probability of token X_i , which is modeled by the language model LM , given the previous tokens and the context S . Similarly, we represent the tokens in a fake sequence sampled by GQS as Y_1, \dots, Y_n .

GQS partitions the next token distribution into $\frac{1}{\epsilon'}$ bins, where $\epsilon' = \epsilon/n$, and each bin contains tokens with probabilities within $[m\epsilon', (m+1)\epsilon']$, where m is the bin index. Since GQS samples Y_i from the same bin as X_i , it is true that $|f(X_i) - f(Y_i)| < \epsilon'$ for all i .

Finally, we can bound the difference between the probability of the target sequence, $\prod_{i=1}^n f(X_i)$, and the probability of the fake sequence, $\prod_{i=1}^n f(Y_i)$, as $n\epsilon' = \epsilon$, using Lemma 9.1. That is,

$$\left| \prod_{i=1}^n f(X_i) - \prod_{i=1}^n f(Y_i) \right| < \epsilon$$

This is true for every pair of target and fake subsequences. Based on Definition 2.1, since the maximum difference between the probabilities (modeled by \mathcal{D}_{LM}) of any target and fake subsequences is ϵ , the two sets of subsequence are ϵ -close over \mathcal{D}_{LM} .

Part II Let us denote the subsequence S_{target} as s , and a fake n-gram sampled by GQS as s' . According to **Part I** and the definitions in §2.3.2, we have

$$\begin{aligned} |P_{\mathcal{D}}(s) - P_{\mathcal{D}}(s')| &= |P_{\mathcal{D}}(s) - P_{\mathcal{D}_{LM}}(s) + P_{\mathcal{D}_{LM}}(s) - P_{\mathcal{D}_{LM}}(s') \\ &\quad + P_{\mathcal{D}_{LM}}(s') - P_{\mathcal{D}}(s')| \\ &\leq |P_{\mathcal{D}}(s) - P_{\mathcal{D}_{LM}}(s)| + |P_{\mathcal{D}_{LM}}(s) - P_{\mathcal{D}_{LM}}(s')| \\ &\quad + |P_{\mathcal{D}_{LM}}(s') - P_{\mathcal{D}}(s')| \\ &\leq \epsilon + 2\Delta. \end{aligned}$$

This is true for every pair of target and fake subsequences. Based on Definition 2.1, since the maximum difference between the probabilities (modeled by \mathcal{D}) of any target and fake subsequences is $\epsilon + 2\Delta$, the two sets of subsequences are $(\epsilon + 2\Delta)$ -close over \mathcal{D} .

9.3. Dataset Preparation for PO

For the evaluation of PO, we selected the initial 500 entries from clinical dialogue datasets and 1500 entries from USMLE Step 2 passages. Since the initial datasets were not tagged with PII information, we used ChatGPT to automatically tag HIPAA-sensitive information according to the guidelines from [53], along with its PII category. Each entry in these datasets averaged 13 redacted PII segments. An example of a dataset item is shown in Figure 15. For the resume dataset, we extracted the first 1500 entries and used Google Cloud’s PII filtering tool to annotate personal information, resulting in an average of 18 PII segments per entry. An anonymized example is presented in Figure 16.

Example Output from GQS. For demonstration, we present the result of running GQS on the name “Mrs. Loraine Wicks”

in Figure 15, sampled with $\epsilon = 1/32$ and $\lambda_{\text{max}} = 512$. Due to space constraints, only the first 30 outputs are shown.

1) Mrs.	Warner	21) Mrs.
Lorraine	Martin	Lillian
Wicks	Thompson	Winter
2) Mrs.	Lorraine	Lillian
Lillian	Brown	Abraham
Brown	Wood	Lillian
3) Mrs.	Lorraine	Cooper
Lorraine	Park	24) Mrs. Lydia
Park	4) Mrs. Lydia	Davis
5) Mrs. Lydia	Jackson	25) Mrs.
Williams	6) Mrs.	Lillian Kim
7) Mrs. Wilson	Lillian	26) Mrs.
8) Mrs. Lydia	Thomas	Lillian
Grant	7) Mrs. Wilson	Thompson
9) Mrs.	Jenkins	27) Mrs. Lydia
Lillian	Lillian	White
Taylor	18) Mrs.	28) Mrs.
10) Mrs. Lydia	Watson	Lillian
Green	19) Mrs.	Davis
11) Mrs.	Lillian	29) Mrs.
Lorraine	Anderson	Lillian
	20) Mrs.	Carter
	Lorraine	30) Mrs.
	Williams	Lorraine
		Miller

[AGE] 17-year-old [GENDER] male, has come to the [ORGANIZATION NAME] student health clinic complaining of [DISEASE] heart pounding. [PERSON NAME] Mrs. Loraine Wicks mother has given verbal consent for a history, physical examination, and treatment - began [DATES] 2-3 months ago, sudden, intermittent for [DATES] 2 days (lasting 3-4 min), worsening, non-allev/aggrav - associated with dyspnea on exertion and rest, stressed out about school - reports he feels like his heart is jumping out of his chest - ROS: denies chest pain, diaphoresis, weight loss, chills, fever, nausea, vomiting, pedal edema - PMH: none, meds: Adderall (from a friend), NKDA - FH: father had MI recently, mother has thyroid disease - SH: non-smoker, marijuana [DATES] 5-6 months ago, 3 beers on the weekend, basketball at school - SH: no STD.

Figure 15: Example entry from the clinical dataset. Yellow-masked text indicates redacted information, with brackets denoting its PII category.

Resume Wizard [PERSON NAME] Jane Doe E-Mail: [EMAIL] jane.doe@example.com Phone: [ID] (123) 456-7890 (M) [ORGANIZATION NAME] Finance & Accounts, Costing Profile Introduction

- A dynamic professional with a qualitative experience of [AGE] 3 years 2 months in the areas of Finance & Accounts, Product Costing & MIS Reporting.
- Presently working as PROCESS LEAD at [ORGANIZATION NAME] Tech Solutions Inc.
- Previously worked as LEAD F&A OPERATIONS at [ORGANIZATION NAME] Global Tech with [ORGANIZATION NAME] Soft Drinks Co Project from [DATES] 1st April 2018 to [DATES] 30th June 2019.
- Involved in the standardization of process & MIS reporting files and contributed a higher rate of organic growth.
- An effective communicator with excellent relationship-building & interpersonal skills. Strong analytical, problem-solving & organizational abilities.
- Areas of interest include budgeting & preparation of AOP (Annual Operating Plans).
- Familiar with SAP FICO modules, MS Office tools.

Figure 16: Example entry from the resume dataset. Note that we anonymized this example with placeholders such as “Jane Doe.” and “(123) 456-7890” for privacy.